Pesticide Biochemistry and Physiology 201 (2024) 105901

Contents lists available at ScienceDirect

Pesticide Biochemistry and Physiology

journal homepage: www.elsevier.com/locate/pest

Multiple lysine substitutions in the peptaibol trichogin GA IV enhance the antibiotic activity against plant pathogenic *Pseudomonas syringae*

Sihem Fodil [a], Marta De Zotti [b,*], Silvio Tundo [c,d], Laura Gabbatore [b], Irene Vettorazzo [b], Simone Luti [e], Rita Musetti [c], Luca Sella [c], Francesco Favaron [c], Ivan Baccelli [a,*]

[a] Institute for Sustainable Plant Protection, National Research Council of Italy, Via Madonna del Piano 10, 50019 Sesto Fiorentino, Italy
[b] Department of Chemistry, University of Padova, Via Marzolo 1, 35131 Padova, Italy
[c] Department of Land, Environment, Agriculture, and Forestry (TESAF), University of Padova, Viale Dell' Università 16, 35020 Legnaro, Italy
[d] Department of Agronomy, Food, Natural Resources, Animals and Environment (DAFNAE), University of Padova, Viale Dell' Università 16, 35020 Legnaro, Italy
[e] Department of Experimental and Clinical Biomedical Sciences, University of Florence, Viale Morgagni 50, 50134 Firenze, Italy

ARTICLE INFO

Keywords:
Pathovar *tomato*
Pathovar *actinidiae*
Biovar 3
Trichoderma longibrachiatum
Peptaibiotic
Antimicrobial peptide

ABSTRACT

Plant diseases caused by *Pseudomonas syringae* are essentially controlled in the field with the use of copper-based products and antibiotics, raising environmental and safety concerns. Antimicrobial peptides (AMPs) derived from fungi may represent a sustainable alternative to those chemicals. Trichogin GA IV, a non-ribosomal, 11-residue long AMP naturally produced by the fungus *Trichoderma longibrachiatum* has the ability to insert into phospholipidic membranes and form water-filled pores, thereby perturbing membrane integrity and permeability. In previous studies, peptide analogs modified at the level of specific residues were designed to be water-soluble and active against plant pathogens. Here, we studied the role of glycine-to-lysine substitutions and of the presence of a C-terminal leucine amide on bioactivity against *Pseudomonas syringae* bacteria. *P. syringae* diseases affect a wide range of crops worldwide, including tomato and kiwifruit. Our results show that trichogin GA IV analogs containing two or three Gly-to-Lys substitutions are highly effective *in vitro* against *P. syringae* pv. *tomato* (*Pst*), displaying minimal inhibitory and minimal bactericidal concentrations in the low micromolar range. The same analogs are also able to inhibit *in vitro* the kiwifruit pathogen *P. syringae* pv. *actinidiae* (*Psa*) biovar 3. When sprayed on tomato plants 24 h before *Pst* inoculation, only tri-lysine containing analogs were able to significantly reduce bacterial titers and symptom development in infected plants. Our results point to a positive correlation between the number of lysine substitutions and the antibacterial activity. This correlation was supported by microscopy analyses performed with mono-, di- and tri-Lys containing analogs that showed a different degree of interaction with *Pst* cells and ultrastructural changes that culminated in cell lysis.

1. Introduction

The genus *Pseudomonas* was described for the first time in 1894 and it is nowadays the bacterial genus containing the highest number of species (> 250) among gram-negative bacteria (Lalucat et al., 2022). The taxon can be divided into two main lineages: *P. aeruginosa* and *P. fluorescens* (Lalucat et al., 2022). *P. pertucinogena*, formerly considered as lineage, has been recently elevated to genus (Rudra and Gupta, 2021; Passarelli-Araujo et al., 2022). The *P. fluorescens* lineage contains six phylogenetic groups, one of those represented by the species *P. syringae* (Passarelli-Araujo et al., 2022). *P. syringae* gives rise to the so-called "*P. syringae* species complex", a phylogenetic group containing various closely related species for a total of >60 pathovars able to cause disease on plants (Gomila et al., 2017).

The *P. syringae* species complex is responsible for causing disease on several economically important monocots and dicots worldwide. Only in the first fifteen years of the present century, it has been associated to >70 disease outbreaks on 40 annual plant species and 55 outbreaks on 25 different woody species (Lamichhane et al., 2014, 2015). On woody species, a relevant example is represented by the devastating kiwifruit (*Actinidia chinensis*) bacterial canker outbreak caused by *P. syringae* pv. *actinidiae* (*Psa*) biovar 3, which started in Italy in 2008 (Balestra et al., 2009; Ferrante and Scortichini, 2009) and spread globally causing severe economic losses especially in Italy, China and New Zealand

* Corresponding authors.
E-mail addresses: marta.dezotti@unipd.it (M. De Zotti), ivan.baccelli@ipsp.cnr.it (I. Baccelli).

https://doi.org/10.1016/j.pestbp.2024.105901
Received 2 February 2024; Received in revised form 5 April 2024; Accepted 6 April 2024
Available online 8 April 2024

(Vanneste, 2017; Donati et al., 2020; Ye et al., 2020). On annual crops, it takes on considerable importance the bacterial speck disease of tomato (*Solanum lycopersicum*), which is caused by *P. syringae* pv. *tomato* (*Pst*) (Kunkeaw et al., 2010). Tomato is the most produced vegetable on a global scale with 189 million tons (FAO, 2022) and *Pst* can infect fruits and leaves in both greenhouse- and open field-grown tomato plants (Griffin et al., 2017; Quaglia et al., 2021), causing significant seedling and yield losses (up to 25% and 75%, respectively) (Panno et al., 2021). *Pst*, thanks to the ability of the strain DC3000 to infect both tomato and *Arabidopsis thaliana*, has also become a model pathogen for studying molecular plant-pathogen interactions (Xin and He, 2013).

Chemical control means against *P. syringae* diseases in the field essentially rely on the use of copper-based products and, in some non-European countries, antibiotics, for example streptomycin (Panno et al., 2021; Pereira et al., 2021). However, both chemicals have limitations in terms of sustainability and safety, emergence of resistant strains, phytotoxicity and regulatory measures that restrict their use (Preston, 2000; Cameron and Sarojini, 2014; Griffin et al., 2017; Quaglia et al., 2021). For these reasons, alternative means such as those employing biological control agents and resistance inducers have been investigated (Pereira et al., 2021; Quaglia et al., 2021). As chemical alternative, antimicrobial peptides (AMPs) have also been proposed (Cameron and Sarojini, 2014). AMPs, by generally targeting the bacterial cell membrane, are expected to hamper the development of resistance phenomena (Cameron and Sarojini, 2014). In addition, they can offer the advantages of the chemical products in terms of manufacturing and ease of use for farmers.

Trichogin GA IV is an 11-residue AMP belonging to the family of lipopeptaibols that is naturally produced by the fungus *Trichoderma longibrachiatum* (Auvin-Guette et al., 1992). Trichogin GA IV shows helical structure thanks to the presence of α-aminoisobutyric acid (Aib) residues in its sequence (De Zotti et al., 2012a). The molecule is moderately amphiphilic: hydrophobic groups (n-octanoyl and Leu, Ile and Lol aliphatic side chains) are located on one helix face, while four Gly residues constitute on the opposite (poorly) hydrophilic face (Peggion et al., 2003; De Zotti et al., 2012b). The amphiphilic nature of trichogin GA IV is responsible for its capability to insert into microbial phospholipidic membranes and form water-filled pores, thereby perturbing membrane integrity and permeability (Bobone et al., 2013; Smetanin et al., 2014).

In previous studies, we demonstrated that trichogin GA IV can be a precious template for the synthesis of novel plant protection molecules, in that analogs modified at the level of specific residues become water-soluble and show antimicrobial activity against different fungi and bacteria, are resistant to proteolysis and not phytotoxic for plants, and can be degraded to nontoxic amino acids when introduced into the environment (De Zotti et al., 2012b; De Zotti et al., 2020; Sella et al., 2021; Baccelli et al., 2022). Moreover, the analog K5,6-L11 $^{(\#4r)}$ can exert broad-spectrum antimicrobial activity, being effective against some fungi, oomycetes and bacteria (Sella et al., 2021; Baccelli et al., 2022; Bolzonello et al., 2023; Caracciolo et al., 2023). However, while this analog was highly effective *in vitro* against *Xanthomonas campestris* pv. *campestris*, it showed limited efficacy against *P. corrugata* and *P. savastanoi*, suggesting that *Pseudomonas* species demand a tailored molecular design. No further investigation was however carried out.

In the present work, to provide a novel plant protection molecule based on trichogin GA IV against *P. syringae* diseases, we investigated the contribution of glycine-to-lysine substitutions and of the modification at the C-terminus on bioactivity against *P. syringae* pv. *tomato* and *P. syringae* pv. *actinidiae*. To do so, we used a series of modified analogs, some of them designed in the present work, to perform studies both *in vitro* and *in planta*.

2. Material and methods

2.1. Peptide synthesis

Trichogin GA IV (native sequence) and nine water-soluble trichogin GA IV analogs were produced by solid-phase peptide synthesis as previously described (De Zotti et al., 2020). All the analogs were characterized by one up to three Gly-to-Lys substitutions with positional differences so as to confer water-solubility (Lys is positively charged) (De Zotti et al., 2012b). To reduce the production costs, the relatively expensive C-terminal leucinol (Lol) moiety was replaced with a Leu-NH_2 (leucine amide) residue in four full-length analogs (De Zotti et al., 2020). To reinforce helicity, one analog carried a further Aib residue in place of Gly (De Zotti et al., 2012a). The purity of the peptides was checked by analytical HPLC as described in previous studies (De Zotti et al., 2020; Baccelli et al., 2022), yielding values >95%. Three fluorescent analogs bearing one (Dalzini et al., 2016), two and three Gly-to-Lys substitutions (#22^{-FITC}, 4^{-FITC} and 5^{-FITC}, respectively) were produced by conjugation with Fluorescein Isothiocyanate (FITC) at the C-terminus, as described in Dalzini et al. (2016). The peptides 4^{-FITC} and 5^{-FITC}, synthesized for the first time in this study, were characterized by HPLC and mass spectrometry (Figs. S1-S6). The peptides were lyophilized for long term storage at −20 °C and solubilized in sterile distilled water to a final concentration of 1 mM upon first use. Because of its poor water solubility, the native trichogin GA IV was first solubilized in 5% ethanol and then diluted in sterile distilled water. All peptide sequences used in this work are reported in Table 1.

Table 1
Trichogin GA IV analogs tested in the present study.

Modifications[a]	Analog no. (#)[b]	Sequence[c]	Synthesis
–	–	1-octanoyl-Aib-Gly-Leu-Aib-Gly-Gly-Leu-Aib-Gly-Ile-Lol	De Zotti et al., 2009
K9	25*	1-octanoyl-Aib-Gly-Leu-Aib-Gly-Gly-Leu-Aib-**Lys**-Ile-Lol	Baccelli et al., 2022
K6	22**	1-octanoyl-Aib-Gly-Leu-Aib-Gly-**Lys**-Leu-Aib-Gly-Ile-Lol	De Zotti et al., 2020
K6-L11	22r	1-octanoyl-Aib-Gly-Leu-Aib-Gly-**Lys**-Leu-Aib-Gly-Ile-**Leu-NH_2**	Sella et al., 2021
K5-U6	6	1-octanoyl-Aib-Gly-Leu-Aib-**Lys**-**Aib**-Leu-Aib-Gly-Ile-Lol	De Zotti et al., 2020
K5,6	4	1-octanoyl-Aib-Gly-Leu-Aib-**Lys**-**Lys**-Leu-Aib-Gly-Ile-Lol	De Zotti et al., 2020
K5,6-L11	4r	1-octanoyl-Aib-Gly-Leu-Aib-**Lys**-**Lys**-Leu-Aib-Gly-Ile-**Leu-NH_2**	De Zotti et al., 2020
K2,5,9	5	1-octanoyl-Aib-**Lys**-Leu-Aib-**Lys**-Gly-Leu-Aib-**Lys**-Ile-Lol	Sella et al., 2021
K2,5,9-L11	5r	1-octanoyl-Aib-**Lys**-Leu-Aib-**Lys**-Gly-Leu-Aib-**Lys**-Ile-**Leu-NH_2**	Caracciolo et al., 2023
K2,5,6-L11	24r	1-octanoyl-Aib-**Lys**-Leu-Aib-**Lys**-**Lys**-Leu-Aib-Gly-Ile-**Leu-NH_2**	Caracciolo et al., 2023
Fluorescent analogs			
K6^{-FITC}	22^{-FITC}	1-octanoyl-Aib-Gly-Leu-Aib-Gly-**Lys**-Leu-Aib-Gly-Ile-**Leu-NH-$(CH_2)_2$-NH-FITC**	Dalzini et al., 2016
K5,6^{-FITC}	4^{-FITC}	1-octanoyl-Aib-Gly-Leu-Aib-**Lys**-**Lys**-Leu-Aib-Gly-Ile-**Leu-NH-$(CH_2)_2$-NH-FITC**	This work
K2,5,9^{-FITC}	5^{-FITC}	1-octanoyl-Aib-**Lys**-Leu-Aib-**Lys**-Gly-Leu-Aib-**Lys**-Ile-**Leu-NH-$(CH_2)_2$-NH-FITC**	This work

[a] Symbol of the amino acid(s) introduced into the sequence and relative position(s) as compared to native trichogin GA IV; commas separate multiple substitutions with the same amino acid; U, Aib, α-aminoisobutyric acid.

[b] Number assigned to the analogs in previous studies; r, rink, refers to rink-amide resin used for peptide synthesis. *the no. 25 was assigned by Caracciolo et al. (2023); **the no. 22 was assigned by Sella et al. (2021), while De Zotti et al. (2020) refers to this analog as the no. 5;

[c] Modifications to the native trichogin GA IV sequence are highlighted in bold; Lol, leucinol; Leu-NH_2, leucine amide; FITC, fluorescein isothiocyanate.

2.2. Bacterial strains and cultivation

The plant pathogens *Pseudomonas syringae* pv. *tomato* strain DC3000 (*Pst* DC3000, rifampicin resistant) (Xin and He, 2013) which causes bacterial speck disease in both tomato and *Arabidopsis*, and *Pseudomonas syringae* pv. *actinidiae* biovar 3 strain KL103 (*Psa* KL103) (Luti et al., 2021), which causes canker in kiwifruit, were grown in King's B liquid medium (1.5 g/L $MgSO_4$*$7H_2O$, 1.5 g/L K_2HPO_4, 10 mL/L glycerol, 20 g/L peptone) at 28 °C. The growth media for *Pst* DC3000 were always supplemented with 50 mg/L rifampicin.

2.3. Screening for antibacterial activity in vitro

The ability of the peptides to inhibit bacterial growth *in vitro* was first assessed against *Pst* DC3000 in 15 mL conical tubes, containing 2 mL King's B liquid medium and each peptide at the final concentrations of 1, 10 or 25 μM. King's B medium only was used as a control, and three replicates per condition were prepared. To ensure equal bacterial inoculum among replicates and concentrations, the tubes were prepared by dispensing King's B medium from a single 30 mL batch previously inoculated with 60 μL of an overnight bacterial culture ($OD_{600\ nm} \approx 0.2$). Bacterial growth was measured with an Easyspec spectrophotometer (Safas, Monaco, France) at 600 nm after 17 h of incubation at 28 °C, 120 rpm. The four most effective peptides against *Pst* DC3000 were subsequently tested against *Psa* KL103 according to the same protocol described above, with the only difference that *Psa* KL103 growth was measured after 22 h of incubation at 28 °C, 120 rpm. Different incubation times were decided on the basis of preliminary data (Fig. S7) in order to stop the assays during the exponential phases of growth. Growth percent values relative to control were calculated by using the absorbance values at 600 nm.

2.4. Determination of minimal inhibitory concentrations (MICs) and minimal bactericidal concentrations (MBCs)

The four most effective antibacterial peptides, as resulting from the previous screenings on *Pst* DC3000 and *Psa* KL103, were subjected to precise determination of the minimal inhibitory concentration (MIC) and minimal bactericidal concentration (MBC) against *Pst* DC3000. The MIC assay was performed in 96-well microplates containing 180 μL King's B liquid medium and 20 μL of 1:2 serial dilutions of the peptides previously prepared at a concentration ten times higher in water. In this way, the peptides were tested for MIC at the final concentrations of 100, 50, 25, 12.5, 6.25, 3.125, 1.5625 and 0.78125 μM. King's B medium supplemented with 20 μL sterile distilled water was used as a control. To ensure equal bacterial inoculum among replicates and concentrations, the King's B medium was dispensed into the wells from a single 15 mL batch previously inoculated with 15 μL of overnight *Pst* DC3000 culture, in line with the screening previously performed. King's B not inoculated was also dispensed into three wells as negative control. All the assays were performed in three technical replicates. The microplates were automatically read in a Synergy H1 Hybrid Multi-Mode Microplate Reader (BioTek, Agilent, CA, USA) every 15 min., at 600 nm, over a period of 42 h, with incubation conditions set as 28 °C and continuous orbital shaking (355 cpm). These conditions were selected after a preliminary growth kinetic experiment performed with both *Pst* DC3000 and *Psa* KL103 (Fig. S8). The value identified as MIC was the lowest peptide concentration able to completely suppress *Pst* DC3000 growth. To determine MBC, 20 μL from each well containing MIC and higher concentrations, plus control, were plated on King's B agar (prepared as described above, plus 15 g/L agar) not supplemented with the peptides, and incubated at 28 °C. After 72 h, the plates were inspected for visible growth and the lowest peptide concentration showing absence of growth recovery was identified as the MBC.

To compare the bactericidal activity of the peptides with that of control agents authorized in agriculture on tomato against *P. syringae*, two commercial products were tested: Verderame 20 WG (Zapi Garden, Italy), containing 20% *w/w* copper sulfate neutralized with calcium hydroxide (Bordeaux mixture), and Biocobre Rame 50 (Alfenatura, Italy), containing 49.3% *w/w* copper oxychloride with calcium carbonate. The recommended doses for tomato, according to the manufacturer, are 4–6 g/L for Verderame 20 WG and 1.2 g/L for Biocobre Rame 50. Therefore, the two products were tested *in vitro* against *Pst* DC3000 at the following concentrations: 10, 50, 100, 200, 250, 500, 750, 1000, 1500 mg/L for both products; 2000, 4000 and 6000 mg/L for Verderame 20 WG. The assays were performed in 96-well microplates as described above. After 42 h incubation, 20 μL from each well were plated on King's B agar not supplemented with copper and inspected 3 days later for visible growth.

2.5. Microscopy analyses

Suspensions for microscopy were prepared in 96-well microplates containing King's B liquid medium, 20 μL of *Pst* DC3000 from an overnight culture as described in *2.3*, and the fluorescent peptides 22^{-FITC}, 4^{-FITC} or 5^{-FITC} at the final concentration of 10, 25 or 50 μM. The bacterium was co-incubated with each peptide for 4 h. King's B medium not inoculated with *Pst* DC3000 was dispensed into three wells and used as negative control. All the assays were performed in three replicates. Twenty microliters of suspension were examined under a Leica DM 4 fluorescence microscope (Leica Microsystem, Wetzlar, Germany) equipped with a Leica Application Suite X (LAS X) software platform. Images were generated with a magnification of 40× by either differential interference contrast (DIC) or epifluorescence optics, the latter by using a GFP filter (excitation, 490 nm; emission, 520 nm). Untreated bacterial samples were observed at the same excitation wavelength used for the fluorochrome (490 nm) as visual controls. For transmission electron microscopy (TEM) analysis, bacterial suspensions were co-incubated for 2 h with the peptides 22, 4 or 5. The suspensions were centrifuged (500 rcf, 2 min.) and resuspended in distilled water. Drops (10 μL) containing water suspensions of untreated *Pst* DC3000 cells (control), or cells treated with the peptides 22, 4 or 5 at the final concentration of 10 μM were adsorbed to carbon-formvar coated copper grids for 1 min. at room temperature. Bacterial negative staining was obtained by floating the grids on drops (10 μl) of 3% (*w/v*) uranyl acetate for 1 min. Grids were dried by using filter paper and examined under a FEI Tecnai G^2 TEM (FEI, Eindhoven, The Netherlands) operating at 120 kV.

2.6. Plant treatments and infections

The four most effective antibacterial peptides *in vitro* were assessed for their ability to restrict bacterial infection *in planta*. To this purpose, tomato plants (*Solanum lycopersicum* cv. Marmande) were grown in commercial soil in a growth room under LED lights, as previously described (Baccelli et al., 2022). Two weeks after germination, 6 plants were sprayed with a 10 mL pump atomizer with *ca.* 700 μL/leaf of 50 μM peptide solution in water, whereas six plants were sprayed with sterile distilled water as a control. Plants were sprayed on the adaxial (upper) leaf surfaces. *Pst* DC3000 was inoculated 24 h later by spraying the adaxial leaf surfaces with 1×10^7 colony-forming units (CFUs)/mL in 10 mM $MgCl_2$ containing 0.01% *v/v* Silwet L-77 Ag (Momentive Performance Materials Inc., NY, USA). Bacterial titers were determined shortly after inoculation (*ca.* 2 h) and after 5 days of incubation at 21–24 °C in closed boxes. The appearance of symptoms was routinely checked at the end of the incubation periods. Bacterial titers were determined as follows: leaves were detached, weighed, washed twice in sterile water and ground in 10 mM $MgCl_2$ in order to extract bacterial cells. Serial dilutions (1:10) of the extract were prepared in 10 mM $MgCl_2$, plated on King's B agar containing 50 mg/L rifampicin, and incubated at 28 °C. As soon as CFUs were visible, they were counted and the bacterial load of each replicate was expressed as Log CFU/mg of fresh tissue. All the

experiments were repeated at least twice.

The leaf area affected by bacterial speck symptoms was quantified at the end of a representative experiment by using one of the effective peptides. Pictures were taken on three terminal leaflets per plant (6 plants per condition) before processing for bacterial titers. Leaf area showing water-soaked lesions and total leaf area were quantified by using the software ImageJ. A disease severity value was calculated as follows: Symptomatic leaf area = (Area covered by symptoms/Total leaf area) x 100%.

2.7. Statistical analysis

Bacterial growth data from *in vitro* screenings were analyzed by unpaired *t*-test (peptide concentration *vs.* control) and considered statistically significant at $p < 0.05$. Bacterial titers in planta were similarly analyzed by unpaired *t*-test (treated *vs.* control) and considered statistically significant at $p < 0.05$. Unpaired *t*-test with Welch's correction was used to analyze leaf area values. Graphs and data analysis, including checks for normality and homogeneity of variance, were performed with GraphPad Prism 9 (GraphPad Software Inc., CA, United States).

3. Results

3.1. Ability of trichogin GA IV analogs to inhibit growth of Pseudomonas syringae pathovars

The plant pathogenic bacteria *Pst* DC3000 and *Psa* KL103 were grown in liquid culture in the presence of trichogin GA IV analogs (Table 1), as described in *2.3*. Three different peptide concentrations were initially tested *in vitro* (1, 10 and 25 μM) against the tomato pathogen *Pst* DC3000, main target of the present study. After 17 h of incubation, the growth of *Pst* DC3000 was strongly reduced in the presence of the analogs K2,5,6-L11 $^{(\#24r)}$, K2,5,9 $^{(\#5)}$, K2,5,9-L11 $^{(\#5r)}$ and K5,6 $^{(\#4)}$, as compared to controls (Fig. 1). The growth reduction was statistically significant with concentrations ≥10 μM. The analogs K6 $^{(\#22)}$, K6-L11 $^{(\#22r)}$ and K5,6-L11 $^{(\#4r)}$ led to a limited growth reduction (Fig. 1). Native trichogin GA IV, as well as the analogs K9 $^{(\#25)}$ and K5-U6 $^{(\#6)}$ were not able to inhibit *Pst* DC3000 growth, and a mild growth enhancement could even be detected (Fig. 1).

In light of these results, the four most effective peptides, hereafter simply called with their reference number 24r, 5, 5r and 4, were tested against *Psa* KL103 to investigate the sensitivity of this important *P. syringae* pathovar to our molecules. Growth was measured after 22 h of incubation, since *Psa* KL103 displayed a delayed exponential phase as compared to *Pst* DC3000 (Fig. S7 and S8). Similarly to *Pst* DC3000, *Psa* KL103 was inhibited by all four analogs tested, although the peptide 4 showed efficacy only at the highest concentration tested (25 μM) (Fig. 2).

3.2. Bactericidal efficacy of trichogin GA IV analogs in vitro

In order to precisely determine minimal inhibitory concentrations (MICs) for the four most effective peptides, and detect potential bactericidal activity against *Pst* DC3000, a growth kinetic experiment was performed. *Pst* DC3000 was incubated in the presence of 1:2 serial dilutions (highest concentration 100 μM) of the peptides 24r, 5, 5r and 4. As shown in Fig. 3, the presence in the medium of low concentrations of trichogin GA IV analogs (approximately 3–6 μM) produced the clear effect of retarding growth. Higher concentrations were instead able to completely suppress *Pst* DC3000 growth (Fig. 3). Differences were however observed: the peptides 24r and 5 completely suppressed growth at 12.5 μM, while 5r and 4 completely suppressed growth at 25 μM (Fig. 3). These concentrations were accordingly identified as the MIC values (Table 2).

To determine the bactericidal activity of the analogs, a growth recovery experiment was performed. After a recovery period of 3 days in King's B agar medium not supplemented with the peptides, the bactericidal activity was detectable as follows: for the peptides 24r, 5 and 4, the MBC value corresponded to twice the MIC (Table 2); for the peptide 5r, the MBC value was equal to the MIC (Table 2).

In summary, the peptides 24r and 5 turned out to be the most effective analogs against *Pst* DC3000 in terms of MIC (12.5 μM). However, the tri-substituted Lys-containing analogs 24r, 5 and 5r were all equally effective in terms of bactericidal activity (MBC 25 μM, corresponding to 34.7–35 mg/L depending on the analog considered). In contrast, the analog 4, containing two Gly-to-Lys substitutions, turned out to be the least effective peptide (Fig. 3 and Table 2).

Interestingly, the two copper-based products that we tested for

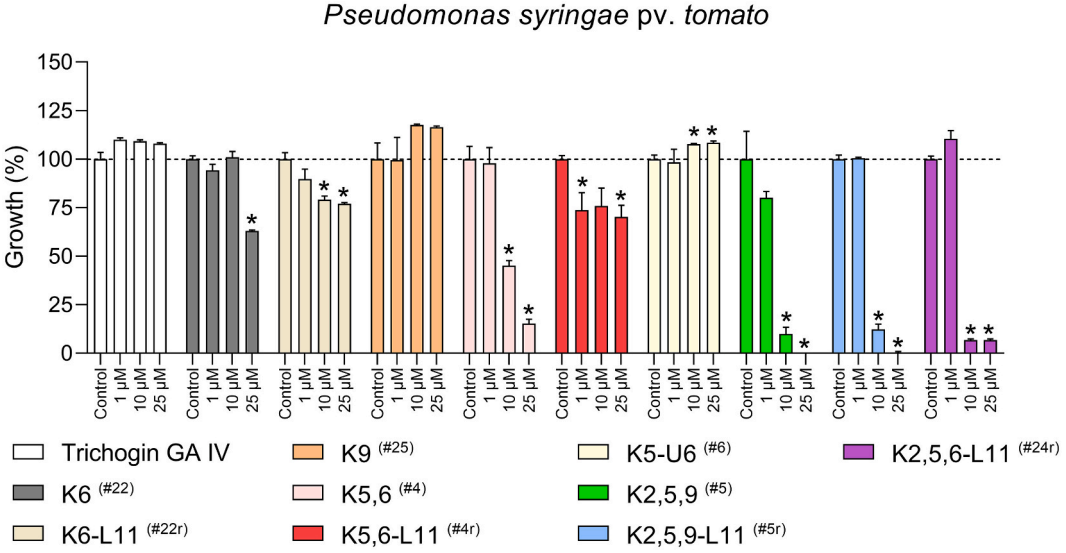

Fig. 1. Efficacy of Trichogin GA IV analogs on *Pseudomonas syringae* pv. *tomato* (*Pst*) DC3000 *in vitro*. *Pst* DC3000 was grown in 2 mL King's B liquid medium in the presence of native Trichogin GA IV (white bars) or different analogs (colored bars) at the final concentration of 1, 10 and 25 μM. King's B medium only was used as control. Incubations were performed at 28 °C, 120 rpm, for 17 h. Growth percent values relative to the corresponding control ± SEM are shown ($n = 3$ biological replicates). Statistically significant differences at $p < 0.05$ (treatment *vs.* control), as determined by unpaired *t*-test, are marked by asterisks. The analog's number (#) is reported as apex.

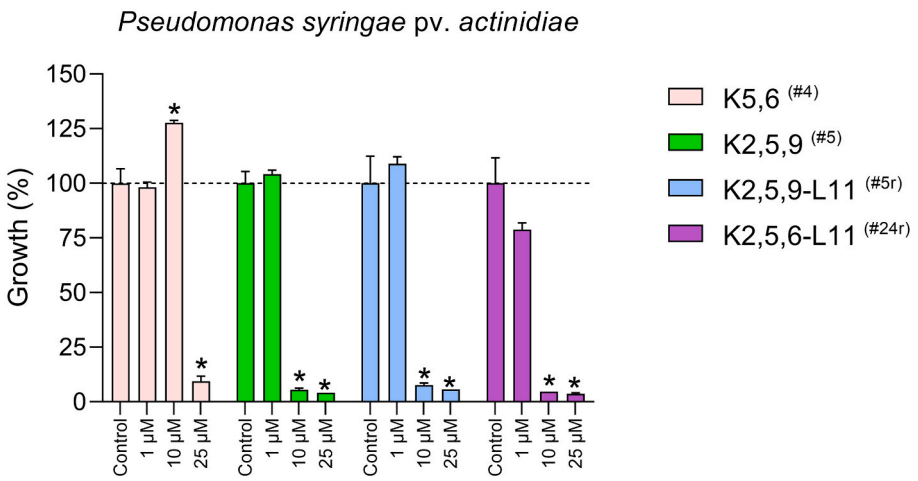

Fig. 2. Efficacy of selected Trichogin GA IV analogs against *Pseudomonas syringae* pv. *actinidiae* (*Psa*) biovar 3, strain KL103, *in vitro*. *Psa* KL103 was grown in 2 mL King's B liquid medium in the presence of the most effective Trichogin GA IV analogs previously shown to inhibit *Pst* DC3000. King's B medium only was used as control. Incubations were performed at 28 °C, 120 rpm, for 22 h. Growth percent values relative to the corresponding control ± SEM are shown (n = 3 biological replicates). Statistically significant differences at $p < 0.05$ (treatment *vs.* control) were determined by unpaired *t*-test and are marked by the asterisk. The analog's number (#) is reported as apex.

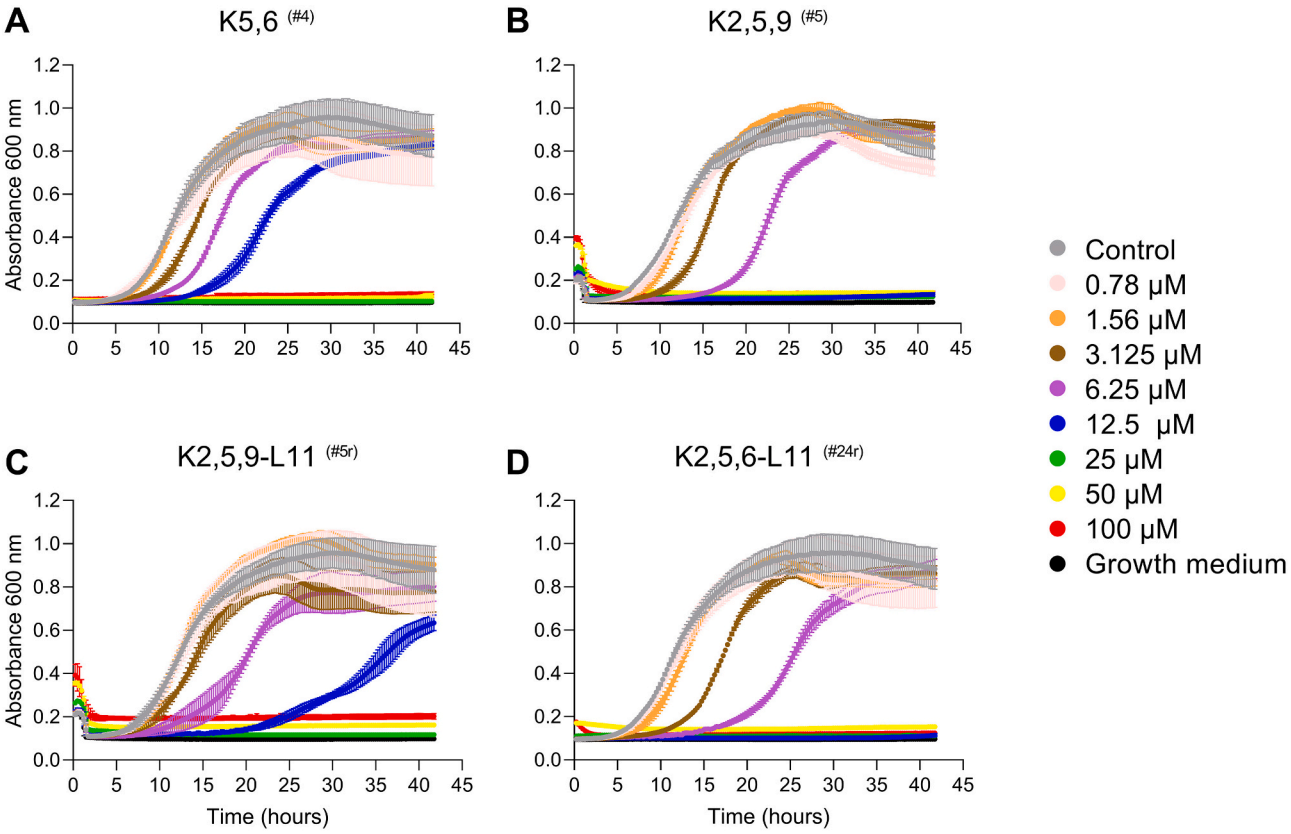

Fig. 3. Growth kinetics of *Pseudomonas syringae* pv. *tomato* (*Pst*) DC3000 at increasing concentrations of inhibiting Trichogin GA IV analogs. Bacteria were grown in a microplate reader in King's B liquid medium containing increasing concentrations of the peptide analogs K5,6 (#4) (**A**), K2,5,9 (#5) (**B**), K2,5,9-L11 (#5r) (C) or K2,5,6-L11 (#24r) (D). Incubations were performed at 28 °C with orbital shaking. The curves show mean absorbance values measured every 15 min ± SD (n = 3 biological replicates). Control (bacterial growth without peptide addition) and culture medium plots are also shown.

comparison were not able to completely kill *Pst* DC3000 cells *in vitro* at the maximum doses recommended for the use on tomato plants in the field (Table S1).

3.3. Interaction of mono-, di- and tri-Lys containing analogs with *P. syringae* cells

The fluorescent analogs $22^{\text{-FITC}}$, $4^{\text{-FITC}}$ and $5^{\text{-FITC}}$, as the analogs representative of one, two and three Gly-to-Lys substitutions, respectively, were subjected to microscopy analyses to investigate the ability

Table 2
Minimal concentrations able to inhibit or kill *Pseudomonas syringae* pv. *tomato* DC3000 *in vitro*.

Trichogin GA IV analog	Analog no. (#)	Minimal Inhibitory Concentration (MIC)[a]	Minimal Bactericidal Concentration (MBC)[b]
K2,5,6-L11	24r	12.5 μM	25 μM
K2,5,9	5	12.5 μM	25 μM
K2,5,9-L11	5r	25 μM	25 μM
K5,6	4	25 μM	50 μM

[a] As resulting from the growth kinetic assay shown in Fig. 3.
[b] As resulting from the growth recovery assay described in Materials and Methods; MBC values were determined after 3 days of incubation in King's B agar plates free of peptide at 28 °C.

of the molecules to interact with bacterial cells. While untreated *Pst* DC3000 cells did no exhibit autofluorescence (Fig. 4A), cells co-incubated with the tri-substituted peptide 5^{-FITC} at 10 μM displayed strong fluorescence signals. Bacteria were visible as either single fluorescent cells or multicellular fluorescent aggregates (Fig. 4B). *Pst* DC3000 cells co-incubated with the di-substituted peptide 4^{-FITC} at 10 μM also showed fluorescence signals, but multicellular aggregates were not present (Fig. 4C). However, bacterial aggregates became visible when cells were co-incubated with a higher concentration (50 μM) (Fig. 4D). No fluorescence signal could instead be observed in the presence of the mono-substituted peptide 22^{-FITC}, either with 10 or 25 μM (Fig. 4E and F). DIC microscopy images demonstrated a similar distribution pattern of bacterial cells, with multicellular aggregates clearly visible only in samples containing 10 μM of the peptide 5^{-FITC} and 50 μM of the peptide 4^{-FITC} (Fig. S9).

Negative staining of bacterial cells was performed to investigate at the ultrastructural level the effect of the peptide treatment on single *Pst*

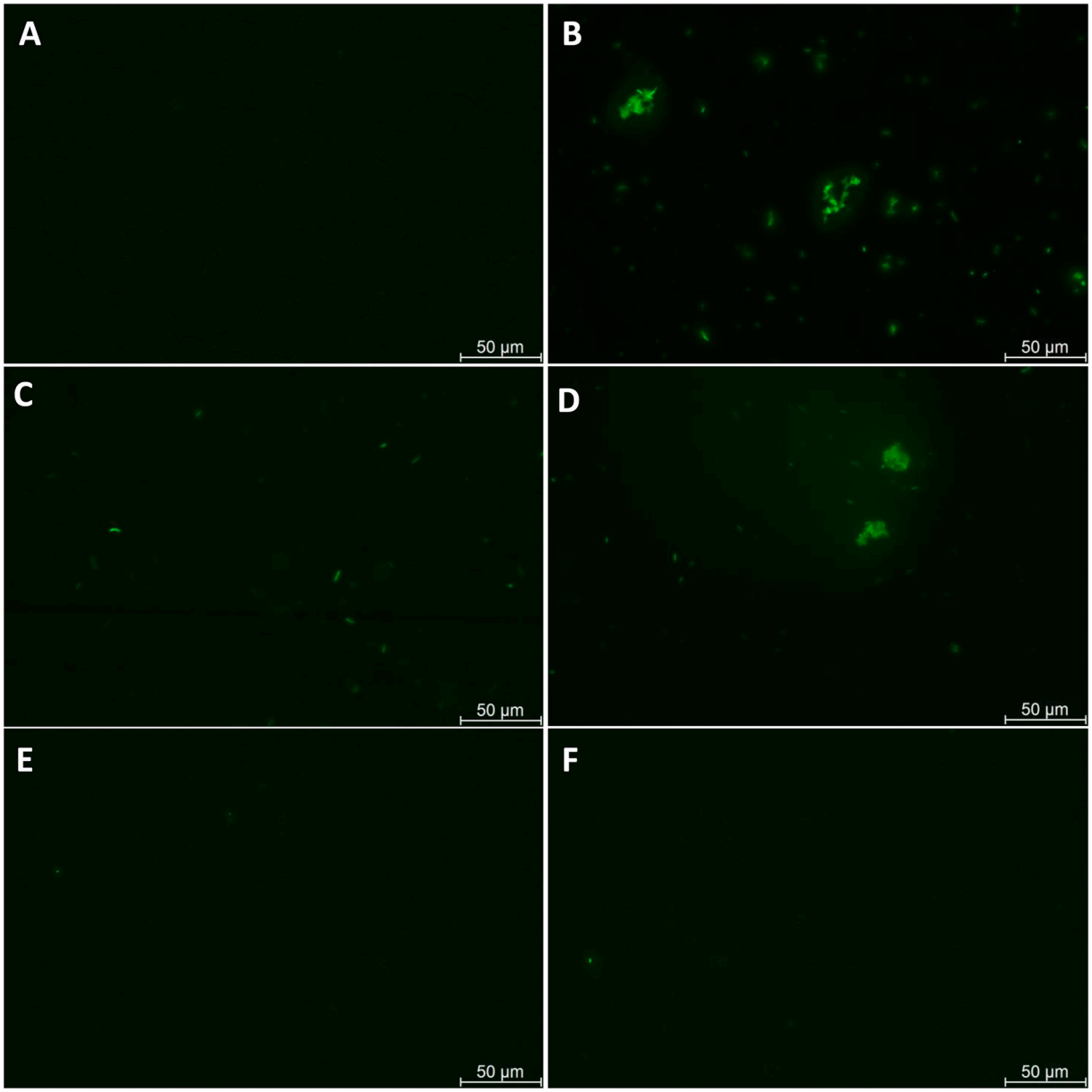

Fig. 4. Fluorescence microscopy of *Pseudomonas syringae* pv. *tomato* DC3000 (*Pst* DC3000) co-incubated with Trichogin GA IV analogs conjugated with the FITC fluorophore. Untreated *Pst* DC3000 cells (**A**), *Pst* cells co-incubated 4 h with the analogs $K2,5,9^{-FITC\ (\#5\text{-}FITC)}$ at 10 μM (B), $K5,6^{-FITC\ (\#4\text{-}FITC)}$ at 10 μM (C) or 50 μM (D), and $K6^{-FITC\ (\#22\text{-}FITC)}$ at 10 μM (E) or 25 μM (F).

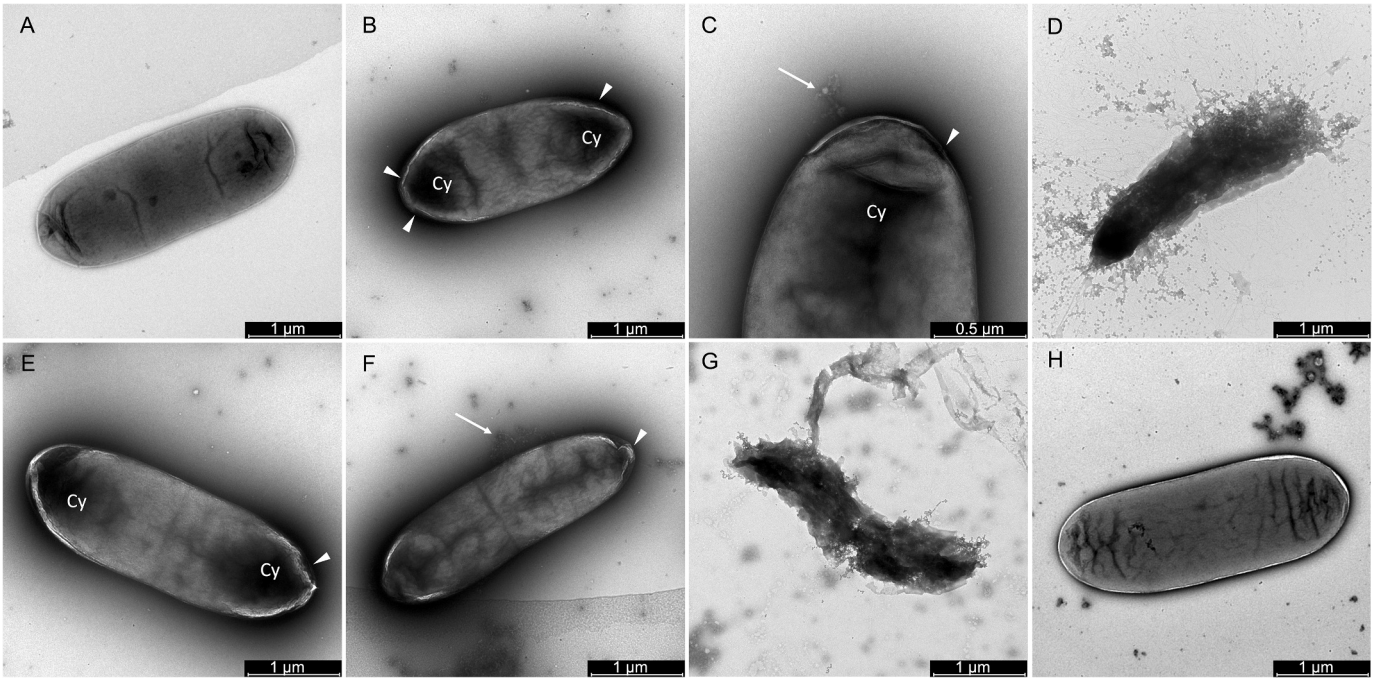

Fig. 5. Representative transmission electron microscopy (TEM) micrographs of *Pseudomonas syringae* pv. *tomato* DC3000 (*Pst* DC3000) co-incubated with Trichogin GA IV analogs. Untreated *Pst* DC3000 cell (**A**), *Pst* cell co-incubated 2 h with the analogs K2,5,9 $^{(\#5)}$ (B, C and D), K5,6 $^{(\#4)}$ (E, F and G) or K6 $^{(\#22)}$ (H) at the concentration of 10 µM. Cells treated with the peptides K5,6 $^{(\#4)}$ and K2,5,9 $^{(\#5)}$ show outer membrane damage (B, C, E and F, arrowheads) cytoplasm condensation (B, C, E, Cy), cytosol leakage (C and F, arrows) and lysis (D and G).

DC3000 cells. TEM analysis revealed that, in comparison with the untreated control (Fig. 5A), huge ultrastructural changes were visible following treatment with the peptides 4 and 5 at 10 µM (Fig. 5B-5G). Treated *Pst* DC3000 cells showed alteration of the outer membrane (Fig. 5B, C, E and F), cytoplasmic condensation (Fig. 5B, C and E), and cytosol leakage (Fig. 5C and F). Moreover, some completely lysed cells were visible (Fig. 5D and G). In contrast, cells treated with the peptide 22 showed fairly conserved morphology (Fig. 5H).

3.4. Tri-Lys-containing analogs reduce bacterial titers and symptom development in infected leaves

Two-week-old tomato plants were leaf-sprayed with a 50 µM peptide solution to evaluate the plant protection efficacy of the four most effective analogs: 24r, 5, 5r and 4. Compared to the *in vitro* results, this concentration corresponded respectively to four times the MIC and two times the MBC for the peptides 24r and 5; two times both MIC and MBC for the peptide 5r; the MBC value and two times the MIC for the peptide 4 (Table 2). Although exceeding minimal inhibitory values established *in vitro*, the 50 µM concentration was deemed suitable because it does not induce phytotoxic effects on plants, as demonstrated in previous studies (Baccelli et al., 2022; Caracciolo et al., 2023), and takes into account potential losses due to the interaction of the peptide with the leaf surface.

Leaves were inoculated by spraying *Pst* DC3000 24 h after peptide treatment and bacterial titers were determined from leaves 5 days later. As shown in Fig. 6, the peptides 24r, 5 and 5r reduced significantly the bacterial titers in comparison to the untreated controls (approximately 10/20-fold less in terms of CFU/mg). This reduction was reflected in the mitigation of bacterial speck symptoms appearing on leaves (Fig. 7). In contrast, the peptide 4 was not able to significantly reduce the bacterial titer in infected plants (Fig. 6) even when tested at double concentration (data not shown).

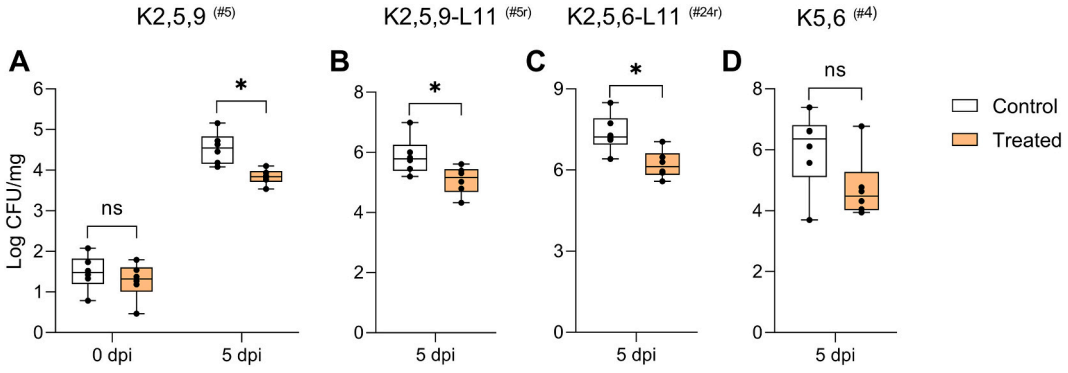

Fig. 6. Tomato plants treated with tri-substituted Lys-containing analogs show reduced bacterial titers. *Pseudomonas syringae* pv. *tomato* (*Pst*) DC3000 was inoculated on *Solanum lycopersicum* cv. Marmande leaves 24 h after treatment with 50 µM peptide K2,5,9 $^{(\#5)}$ (**A**), K2,5,9-L11 $^{(\#5r)}$ (**B**), K2,5,6-L11 $^{(\#24r)}$ (**C**) and K5,6 $^{(\#4)}$ (**D**). Boxes and whiskers include the values obtained from six plants per treatment ($n = 6$). Statistically significant differences at $p < 0.05$ (*) were determined by unpaired *t*-test. Similar results were obtained in two independent experiments. ns, not significant; dpi, days post bacterial inoculation.

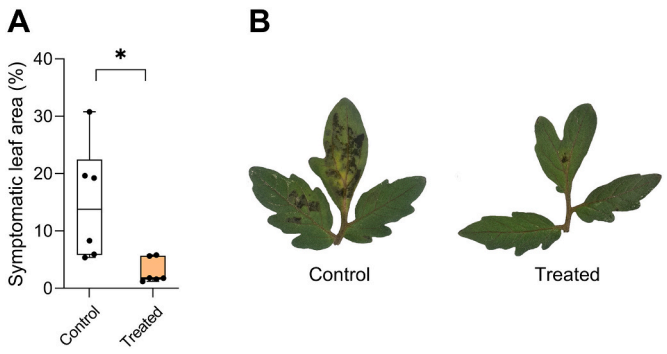

Fig. 7. Bacterial speck symptoms on tomato leaves treated with a tri-Lys analog. Leaf area affected by bacterial speck symptoms in plants treated with 50 μM K2,5,9-L11 $^{(\#5r)}$, or water as control, 5 days post inoculation (dpi) with *Pst* DC3000 (**A**). Six plants per condition were analyzed (n = 6). Statistically significant differences at $p < 0.05$ (*) were determined by unpaired *t*-test with Welch's correction (n = 6). Representative pictures of bacterial speck symptoms in control and treated leaves at 5 dpi (**B**).

4. Discussion

In medical and agricultural sciences there is a common need to develop novel molecules to treat bacterial infections. In medicine, new antibiotics are urgently needed to address the issue of antibiotic resistance (Dalla Torre et al., 2023). In agriculture, antibiotic resistance of plant pathogenic bacteria is only part of the problem (Sundin and Wang, 2018), because antibiotics are forbidden in many countries as plant protection products. In addition, legislation requirements and environmental concerns impose constraints on the use and availability of chemicals for plant protection. In this scenario, trichogin GA IV analogs have attracted increasing attention in recent years, because they have proven effective *in vitro* against antibiotic-resistant human pathogenic bacteria, such as the Gram-positive *Staphylococcus aureus* and the Gram-negative *Acinetobacter baumannii* and *P. aeruginosa* (Tavano et al., 2016; Dalla Torre et al., 2023), and can protect plants from the pathogenic bacterium *X. campestris* pv. *campestris* (*Xcc*) (Caracciolo et al., 2023).

With this study, we broaden the spectrum of efficacy of trichogin analogs for sustainable plant disease protection by demonstrating, *in vitro* and *in planta*, the antibiotic efficacy of lysine-containing trichogin GA IV analogs against Gram-negative plant pathogenic *P. syringae* bacteria. In addition, we highlight chemical features of the analogs that are crucial for the bactericidal activity against *P. syringae*, so as to provide a background of knowledge which will be essential for designing novel plant protection products inspired by trichogin GA IV.

As mentioned in the introduction, streptomycin and copper-based products are used around the globe to treat *P. syringae* infections in agriculture. Lee et al. (2005) reports that copper sulfate has MIC values of 500 μM on several *P. syringae* strains, whereas MIC values for streptomycin sulfate range approximately from 7 to 345 μM depending on the strain (Lee et al., 2005). Two 8-residue AMPs described by Zhang et al. (2023) as innovative antibacterial agents against *Psa*, Jelleine-I and its derivative Jelleine-Ic, have MIC values of 26 and 2.7 μM (originally expressed as μg/mL), respectively. Our best performing analogs had MIC values of 12.5 μM and inhibited *in vitro* the growth of both *Pst* and *Psa*.

Copper-based products, such as copper sulfate and copper oxychloride that we tested for comparison in this study, are not able to completely kill *Pst* DC3000 at the maximum doses recommended for the use in the field on tomato plants (Table S1). In contrast, our most effective analogs, *i.e.* the peptides 24r, 5 and 5r, all containing three lysine residues replacing glycine, showed bactericidal activity *in vitro* against *Pst* DC3000 at 25 μM (corresponding to 34.7–35 mg/L depending on the analog considered), and showed preventive efficacy against *Pst* infection in tomato plants by reducing bacterial titer and mitigating symptom development. The peptide 4, with only two Gly-to-Lys substitutions, exhibited two-fold higher MBC (50 μM) (Table 2) and did not significantly reduce bacterial titers in treated plants. Peptide analogs with only one Gly-to-Lys substitution displayed either no efficacy or limited effectiveness (Fig. 1), while native trichogin GA IV, which does not contain lysine residues, was not effective *in vitro* against *Pst* at the tested concentrations (≤25 μM) (Fig. 1). Tavano et al. (2015) reported the absence of inhibiting activity of native trichogin against *P. aeruginosa* at concentrations ≤64 μM, in line with our data. However, our results point to a direct correlation between the number of Gly-to-Lys substitutions and the antibacterial activity of the peptides, as a probable consequence of their enhanced amphiphilicity (De Zotti et al., 2012b).

The enhanced amphiphilicity of the peptide is expected to increase its ability to form pores, enter the bacterial membranes and thereby exert toxic activity. In accordance with this expectation, the microscopy analyses revealed correlation between the number of lysine substitutions and the level of interaction with *Pst* cells, as highlighted by the greater fluorescence of the sample (Fig. 4). When *Pst* cells were indeed incubated with the fluorescent peptide $5^{\text{-FITC}}$ containing three lysines, a more intense and widespread labeling of the sample was visible as compared to the incubation with $4^{\text{-FITC}}$ and $22^{\text{-FITC}}$ at the same concentration, suggesting greater internalization of the peptide by the *Pst* cells. Moreover, multicellular aggregates were formed only in the presence of the most effective peptide $5^{\text{-FITC}}$, or in the presence of the analog $4^{\text{-FITC}}$ at a concentration five times higher, as a probable consequence of the toxicity of the peptide. The literature suggests indeed that bacterial aggregation is induced by the production of exopolysaccharides and other matrix components as a defense response to environmental stresses, antibiotic treatments (El-shama et al., 2021; Secor et al., 2022) or when cellular growth is inhibited (Tsimring et al., 1995). Therefore, it is reasonable to conclude that *Pst* cells were initiating a cell aggregation process as a direct consequence of the antibacterial activity of the peptides. The TEM analysis actually revealed that ultrastructural modifications take place in *Pst* cells incubated with the peptides 4 and 5 at 10 μM. These changes result in cell lysis and cytosol leakage. Again, no visible effect was detectable after incubation with the peptide 22 (Fig. 5).

In our study, the relative position of the third lysine residue within the sequence also appeared to be important for the antibacterial activity against *Pst*: the analog 5r, presenting the third Lys residue at position 9 (K2,5,9-L11), showed a MIC of 25 μM, whereas the analog 24r bearing the third Lys at position 6 (K2,5,6-L11) was more effective (MIC 12.5 μM).

Peptides 5r and 24r were designed to carry a C-terminal leucine amide residue (−Leu-NH_2) instead of the native 1,2-aminoalcohol Lol, a substitution aimed at reducing the synthesis costs for a possible commercial production of the most effective molecules. The observation that the analog 5 (K2,5,9) showed a MIC value of 12.5 μM while the analog 5r (K2,5,9-L11) exhibited a MIC of 25 μM, along with the lower activity shown by the peptide 4r (K5,6-L11) *vs* 4 (K5,6) during the initial screening (Fig. 1), could suggest that the presence of Leu-NH_2 replacing native leucinol negatively influences the antibacterial activity. However, the bactericidal activity of the peptides 5, 5r and 24r occurred at an identical MBC value of 25 μM, and the three analogs were similarly effective in reducing *Pst* multiplication at the concentration used to treat tomato plants. Therefore, we may conclude that a Lol-to-Leu-NH_2 substitution is a viable modification that is not expected to considerably affect the protective efficacy of the molecule during possible on-field applications.

Caracciolo et al. (2023) did not find any relationship between the number of Gly-to-Lys substitutions or the presence of a C-terminal amide with the antibacterial activity of the peptides against *Xcc*. In contrast, Tavano et al. (2016) found enhanced antibiotic activity of di- or tri-lysine containing analogs against the human pathogen *P. aeruginosa*, similarly to what we are reporting. With our data, it seems possible to hypothesize that pseudomonads, thanks to their apparent lower

sensitivity to trichogin analogs as compared to other bacterial species (Tavano et al., 2016; Caracciolo et al., 2023; Dalla Torre et al., 2023), need a more hydrophilic molecule to be damaged.

To conclude, peptides 4 and 4r, previously reported to be highly effective against different plant pathogens, such as the fungi *Botrytis cinerea* (De Zotti et al., 2020; Baccelli et al., 2022) and *Pyricularia oryzae* (Sella et al., 2021), the oomycete *Plasmopara viticola* (Bolzonello et al., 2023) and the bacterium *Xcc* (Caracciolo et al., 2023), were not the best performing analogs against *Pst*. This observation, besides providing further insight for the identification of the best suited analogs against *P. syringae*, strengthens the evidence that an effective treatment of different microorganisms requires tailor-made molecular design. The optimal peptide configuration for *Pseudomonas syringae* was obtained with three Gly-to-Lys substitutions at positions 2, 5 and 6. This peptide can represent a valid ecofriendly weapon towards sustainable plant protection.

Funding

This work was supported by the Italian Ministry for University and Research, PRIN 2017, grant n. 20173LBZM2. The work was also carried out within the Agritech National Research Center receiving funding from the European Union - NextGenerationEU (PIANO NAZIONALE DI RIPRESA E RESILIENZA - PNRR, MISSIONE 4, COMPONENTE 2, INVESTIMENTO 1.4 – D.D. 1032 17/06/2022, CN00000022). This manuscript reflects only the authors' views and opinions, neither the European Union nor the European Commission can be considered responsible for them.

CRediT authorship contribution statement

Sihem Fodil: Writing – original draft, Validation, Investigation, Formal analysis. **Marta De Zotti:** Writing – review & editing, Supervision, Resources, Funding acquisition, Conceptualization. **Silvio Tundo:** Writing – review & editing, Investigation. **Laura Gabbatore:** Resources. **Irene Vettorazzo:** Resources. **Simone Luti:** Investigation. **Rita Musetti:** Writing – review & editing, Investigation. **Luca Sella:** Writing – review & editing, Supervision, Funding acquisition, Conceptualization. **Francesco Favaron:** Writing – review & editing, Supervision, Funding acquisition, Conceptualization. **Ivan Baccelli:** Writing – original draft, Visualization, Supervision, Project administration, Funding acquisition, Formal analysis, Conceptualization.

Declaration of competing interest

The authors declare the absence of any conflict of interest.

Data availability

The data that support the findings of this study are available from the corresponding author upon reasonable request.

Acknowledgments

The authors are grateful to Prof. Guido Marchi, University of Florence, for providing the *Psa* strain KL103.

Appendix A. Supplementary data

Supplementary data to this article can be found online at https://doi.org/10.1016/j.pestbp.2024.105901.

References

Auvin-Guette, C., Rebuffat, S., Prigent, Y., Bodo, B., 1992. Trichogin a IV, an 11-residue lipopeptaibol from *Trichoderma longibrachiatum*. J. Am. Chem. Soc. 114, 2170–2174. https://doi.org/10.1021/ja00032a035.

Baccelli, I., Luti, S., Bernardi, R., Favaron, F., De Zotti, M., Sella, L., 2022. Water-soluble Trichogin GA IV-derived peptaibols protect tomato plants from *Botrytis cinerea* infection with limited impact on plant defenses. Front. Plant Sci. 13, 881961 https://doi.org/10.3389/fpls.2022.881961.

Balestra, G.M., Mazzaglia, A., Quattrucci, A., Renzi, M., Rossetti, A., 2009. Current status of bacterial canker spread on kiwifruit in Italy. Australas. Plant Dis. 4, 34–36. https://doi.org/10.1071/DN09014.

Bobone, S., Gerelli, Y., De Zotti, M., Bocchinfuso, G., Farrotti, A., Orioni, B., Sebastiani, F., Latter, E., Penfold, J., Senesi, R., Formaggio, F., Palleschi, A., Toniolo, C., Fragneto, G., Stella, L., 2013. Membrane thickness and the mechanism of action of the short peptaibol trichogin GA IV. Biochim. Biophys. Acta-Biomembr. 1828, 1013–1024. https://doi.org/10.1016/j.bbamem.2012.11.033.

Bolzonello, A., Morbiato, L., Tundo, S., Sella, L., Baccelli, I., 2023. Echeverrigaray S, Musetti R, De Zotti M and Favaron F. Peptide analogs of a *Trichoderma* peptaibol effectively control downy mildew in the vineyard. Plant Dis. 107, 2643–2652. https://doi.org/10.1094/PDIS-09-22-2064-RE.

Cameron, A., Sarojini, V., 2014. *Pseudomonas syringae* pv. actinidiae: chemical control, resistance mechanisms and possible alternatives. Plant Pathol. 63, 1–11. https://doi.org/10.1111/ppa.12066.

Caracciolo, R., Sella, L., De Zotti, M., Bolzonello, A., Armellin, M., Trainotti, L., Favaron, F., Tundo, S., 2023. Efficacy of *Trichoderma longibrachiatum* Trichogin GA IV peptaibol analogs against the black rot pathogen *Xanthomonas campestris* pv. *campestris* and other phytopathogenic bacteria. Microorganisms 11, 480. https://doi.org/10.3390/microorganisms11020480.

Dalla Torre, C., Sannio, F., Battistella, M., Docquier, J.D., De Zotti, M., 2023. Peptaibol analogs show potent antibacterial activity against multidrug resistant opportunistic pathogens. Int. J. Mol. Sci. 24, 7997. https://doi.org/10.3390/ijms24097997.

Dalzini, A., Bergamini, C., Biondi, B., De Zotti, M., Panighel, G., Fato, R., Peggion, C., Bortolus, M., Maniero, A.L., 2016. The rational search for selective anticancer derivatives of the peptide Trichogin GA IV: a multi-technique biophysical approach. Sci. Rep. 6, 24000. https://doi.org/10.1038/srep24000.

De Zotti, M., Biondi, B., Formaggio, F., Toniolo, C., Stella, L., Park, Y., Hahm, K.S., 2009. Trichogin GA IV: an antibacterial and protease-resistant peptide. J. Pept. Sci. 15, 615–619. https://doi.org/10.1002/psc.1135.

De Zotti, M., Biondi, B., Peggion, C., Formaggio, F., Park, Y., Hahm, K.S., Toniolo, C., 2012a. Trichogin GA IV: a versatile template for the synthesis of novel peptaibiotics. Org. Biomol. Chem. 10, 1285–1299. https://doi.org/10.1039/c1ob06178j.

De Zotti, M., Biondi, B., Park, Y., Hahm, K.S., Crisma, M., Toniolo, C., Formaggio, F., 2012b. Antimicrobial lipopeptaibol trichogin GA IV: role of the three Aib residues on conformation and bioactivity. Amino Acids 43, 1761–1777. https://doi.org/10.1007/s00726-012-1261-7.

De Zotti, M., Sella, L., Bolzonello, A., Gabbatore, L., Peggion, C., Bortolotto, A., Elmaghraby, I., Tundo, S., Favaron, F., 2020. Targeted amino acid substitutions in a *Trichoderma* peptaibol confer activity against fungal plant pathogens and protect host tissues from *Botrytis cinerea* infection. Int. J. Mol. Sci. 21, 7521. https://doi.org/10.3390/ijms21207521.

Donati, I., Cellini, A., Sangiorgio, D., Vanneste, J.L., Scortichini, M., Balestra, G.M., Spinelli, F., 2020. *Pseudomonas syringae* pv. *actinidiae*: ecology, infection dynamics and disease epidemiology. Microb. Ecol. 80, 81–102. https://doi.org/10.1007/s00248-019-01459-8.

El-shama, Q., Nwoko, A., Okeke, I.N., 2021. Bacteria autoaggregation: how and why bacteria stick together. Biochem. Soc. Trans. 49, 1147–1157. https://doi.org/10.1042/BST20200718.

FAO, 2022. Agricultural production statistics 2000–2021. FAOSTAT Analytical Brief Series No. 60. Rome. https://doi.org/10.4060/cc3751en.

Ferrante, P., Scortichini, M., 2009. Identification of *Pseudomonas syringae* pv. *actinidiae* as causal agent of bacterial canker of yellow kiwifruit (*Actinidia chinensis* Planchon) in Central Italy. J. Phytopathol. 157, 768–770. https://doi.org/10.1111/j.1439-0434.2009.01550.x.

Gomila, M., Busquets, A., Mulet, M., García-Valdés, E., Lalucat, J., 2017. Clarification of taxonomic status within the *Pseudomonas syringae* species group based on a phylogenomic analysis. Front. Microbiol. 8, 2422. https://doi.org/10.3389/fmicb.2017.02422.

Griffin, K., Gambley, C., Brown, P., Li, Y., 2017. Copper-tolerance in *Pseudomonas syringae* pv. *tomato* and *Xanthomonas* spp. and the control of diseases associated with these pathogens in tomato and pepper. A systematic literature review. Crop Prot. 96, 144–150. https://doi.org/10.1016/j.cropro.2017.02.008.

Kunkeaw, S., Tan, S., Coaker, G., 2010. Molecular and evolutionary analyses of *Pseudomonas syringae* pv. *tomato* race 1. Mol. Plant-Microbe Interact. 23, 415–424. https://doi.org/10.1094/MPMI-23-4-0415.

Lalucat, J., Gomila, M., Mulet, M., Zaruma, A., García-Valdés, E., 2022. Past, present and future of the boundaries of the *Pseudomonas* genus: proposal of *Stutzerimonas* gen. Nov. Syst. Appl. Microbiol. 45, 126289 https://doi.org/10.1016/j.syapm.2021.126289.

Lamichhane, J.R., Varvaro, L., Parisi, L., Audergon, J.M., Morris, C.E., 2014. Disease and frost damage of woody plants caused by *Pseudomonas syringae*: seeing the forest for the trees. Adv. Agron. 126, 235–295. https://doi.org/10.1016/B978-0-12-800132-5.00004-3.

Lamichhane, J.R., Messéan, A., Morris, C.E., 2015. Insights into epidemiology and control of diseases of annual plants caused by the *Pseudomonas syringae* species

complex. J. Gen. Plant Pathol. 81, 331–350. https://doi.org/10.1007/s10327-015-0605-z.

Lee, J.H., Kim, J.H., Kim, G.H., Jung, J.S., Hur, J.S., Koh, Y.J., 2005. Comparative analysis of korean and japanese strains of *Pseudomonas syringae* pv. *actinidiae* causing bacterial canker of kiwifruit. Plant Pathol. J. 21, 119–126. https://doi.org/10.5423/PPJ.2005.21.2.119.

Luti, S., Campigli, S., Ranaldi, F., Paoli, P., Pazzagli, L., Marchi, G., 2021. Lscβ and lscγ, two novel levansucrases of *Pseudomonas syringae* pv. *actinidiae* biovar 3, the causal agent of bacterial canker of kiwifruit, show different enzymatic properties. Int. J. Biol. Macromol. 179, 279–291. https://doi.org/10.1016/j.ijbiomac.2021.02.189.

Panno, S., Davino, S., Caruso, A.G., Bertacca, S., Crnogorac, A., Mandić, A., Noris, E., Matić, S., 2021. A review of the most common and economically important diseases that undermine the cultivation of tomato crop in the mediterranean basin. Agronomy 11, 2188. https://doi.org/10.3390/agronomy11112188.

Passarelli-Araujo, H., Franco, G.R., Venancio, T.M., 2022. Network analysis of ten thousand genomes shed light on *Pseudomonas* diversity and classification. Microbiol. Res. 254, 126919 https://doi.org/10.1016/j.micres.2021.126919.

Peggion, C., Formaggio, F., Crisma, M., Epand, R.F., Epand, R.M., Toniolo, C., 2003. Trichogin: a paradigm for lipopeptaibols. J. Pept. Sci. 9, 679–689. https://doi.org/10.1002/psc.500.

Pereira, C., Costa, P., Pinheiro, L., Balcão, V.M., Almeida, A., 2021. Kiwifruit bacterial canker: an integrative view focused on biocontrol strategies. Planta 253, 49. https://doi.org/10.1007/s00425-020-03549-1.

Preston, G.M., 2000. *Pseudomonas syringae* pv. *tomato*: the right pathogen, of the right plant, at the right time. Mol. Plant Pathol. 1, 263–275. https://doi.org/10.1046/j.1364-3703.2000.00036.x.

Quaglia, M., Bocchini, M., Orfei, B., D'Amato, R., Famiani, F., Moretti, C., Buonaurio, R., 2021. Zinc phosphate protects tomato plants against *Pseudomonas syringae* pv. *tomato*. J. Plant Dis. Prot. 128, 989–998. https://doi.org/10.1007/s41348-021-00444-z.

Rudra, B., Gupta, R.S., 2021. Phylogenomic and comparative genomic analyses of species of the family *Pseudomonadaceae*: proposals for the genera *Halopseudomonas* gen. nov. and *Atopomonas* gen. nov., merger of the genus *Oblitimonas* with the genus *Thiopseudomonas*, and transfer of some misclassified species of the genus *Pseudomonas* into other genera. Int. J. Syst. Evol. Microbiol. 71 https://doi.org/10.1099/ijsem.0.005011.

Secor, P.R., Michaels, L.A., Bublitz, D.C., Jennings, L.K., Singh, P.K., 2022. The depletion mechanism actuates bacterial aggregation by exopolysaccharides and determines species distribution & composition in bacterial aggregates. Front. Cell. Infect. Microbiol. 12, 869736 https://doi.org/10.3389/fcimb.2022.869736.

Sella, L., Govind, R., Caracciolo, R., Quarantin, A., Vu, V.V., Tundo, S., Nguyen, H.M., Favaron, F., Musetti, R., De Zotti, M., 2021. Transcriptomic and ultrastructural analyses of *Pyricularia oryzae* treated with fungicidal peptaibol analogs of *Trichoderma* trichogin. Front. Microbiol. 12, 753202 https://doi.org/10.3389/fmicb.2021.753202.

Smetanin, M., Sek, S., Maran, F., Lipkowski, J., 2014. Molecular resolution visualization of a pore formed by trichogin, an antimicrobial peptide, in a phospholipid matrix. Biochim. Biophys. Acta-Biomembr. 1838, 3130–3136. https://doi.org/10.1016/j.bbamem.2014.08.006.

Sundin, G.W., Wang, N., 2018. Antibiotic resistance in plant-pathogenic bacteria. Annu. Rev. Phytopathol. 56, 161–180. https://doi.org/10.1146/annurev-phyto-080417-045946.

Tavano, R., Malachin, G., De Zotti, M., Peggion, C., Biondi, B., Fornaggio, F., Papini, E., 2015. The peculiar N- and C-termini of trichogin GA IV are needed for membrane interaction and human cell death induction at doses lacking antibiotic activity. Biochim. Biophys. Acta-Biomembr. 1848, 134–144. https://doi.org/10.1016/j.bbamem.2014.10.005.

Tavano, R., Malachin, G., De Zotti, M., Peggion, C., Biondi, B., Formaggio, F., Papini, E., 2016. Comparison of bactericidal and cytotoxic activities of trichogin analogs. Data Brief 6, 359–367. https://doi.org/10.1016/j.dib.2015.12.006.

Tsimring, L., Levine, H., Aranson, I., Ben-Jacob, E., Cohen, I., Shochet, O., Reynolds, W. N., 1995. Aggregation patterns in stressed bacteria. Phys. Rev. Lett. 75, 1859–1862. https://doi.org/10.1103/PhysRevLett.75.1859.

Vanneste, J.L., 2017. The scientific, economic, and social impacts of the New Zealand outbreak of bacterial canker of kiwifruit (*Pseudomonas syringae* pv. *actinidiae*). Annu. Rev. Phytopathol. 55, 377–399. https://doi.org/10.1146/annurev-phyto-080516-035530.

Xin, X.F., He, S.Y., 2013. *Pseudomonas syringae* pv. *tomato* DC3000: a model pathogen for probing disease susceptibility and hormone signaling in plants. Annu. Rev. Phytopathol. 51, 473–498. https://doi.org/10.1146/annurev-phyto-082712-102321.

Ye, Z.F., Wei, P.F., Xue, S.Z., Liu, P., Jia, B., Heng, W., Zhu, L.W., 2020. Characterization of *Pseudomonas syringae* pv. *actinidiae* Biovar 3 strain and cultivar tolerance to kiwifruit bacterial canker in China. J. Plant Pathol. 102, 443–450. https://doi.org/10.1007/s42161-019-00459-4.

Zhang, M., Wang, L., Tang, W., Xing, Y., Liu, P., Dang, X., 2023. Antibacterial mechanism of the novel antimicrobial peptide Jelleine-Ic and its efficacy in controlling *Pseudomonas syringae* pv. *actinidiae* in kiwifruit. Pest Manag. Sci. 79, 3681–3692. https://doi.org/10.1002/ps.7548.